

Role of Nitrogen in the Formation of HC–N Films by CH₄/N₂ Barrier Discharge Plasma: Aliphatic Tendency

Abhijit Majumdar,^{*,†} Gobind Das,[‡] Kaleswara Rao Basvani,[§] Joachim Heinicke,[§] and Rainer Hippler[†]

Institute of Physics, Ernst-Moritz-Arndt-University Greifswald, Felix-Hausdorff-Str. 6, 17489 Greifswald, Germany, Lab. BIONEM, Università Magna Græcia di Catanzaro, Campus Germaneto, Viale Europa, 88100 Catanzaro, Italy, and Institute for Biochemistry, Ernst-Moritz-Arndt-University Greifswald, Felix-Hausdorff-Str. 4, 17489 Greifswald, Germany

Received: July 14, 2009; Revised Manuscript Received: September 23, 2009

We have studied the influence of nitrogen on the chemical properties of the hydrogenated carbon nitride (a-CN_x:H) film deposited by CH₄/N₂ dielectric barrier discharge (DBD) plasma. X-ray photoelectron spectroscopy (XPS) indicates that carbon and nitrogen form an unpolarized covalent bond in these C–N_x materials, and the observed chemical shift in the C 1s and N 1s binding energy is explained with respect to N 1s incorporation. Furthermore, the average nitrogen content (N/C ≈ 0.76) in the films was systematically varied by changing the nitrogen partial pressure (CH₄/N₂ ≈ from 5:1 to 1:7) which is well supported by the elemental analysis. Fourier transform infrared (FTIR) absorption spectra exhibit significant changes in different C–N, C≡N, and NH/OH molecular bands at higher nitrogen concentration in the film. The isonitrile and nitrile groups (–NC and –CN) are increased with the increase of deposition time. In addition, the elemental analysis, proton NMR, and thermolysis mass spectrum show that the composition of the film with the ratio CH₄/N₂ ≈ 1:1 is C, 67.68; H, 9.88; N, 16.53 (in wt %) and that the film is composed of polymers, probably containing linear chains which are cleaved off on heating in vacuum.

I. Introduction

Hypothetical prediction regarding the mechanical properties superiority of β-C₃N₄ solids to those of diamond^{1–3} has attracted a great interest toward carbon–nitrogen materials. Synthesis and outstanding mechanical properties of C₃N₄ has been claimed by some groups,^{4,5} but still, there is no conclusive evidence about the possibility of synthesizing such super hard crystalline solids. Rather than the super hard materials of carbon (i.e., diamond or β-C₃N₄ phase), the amorphous carbon nitride (a-CN_x) film is expected to be applied widely as, for example, a superhard coating material, and low friction coefficient,^{6–8} low band gap protective material on hard disks and read heads,^{9,10} photoluminescence,¹¹ carbon nitride nanotubes,¹² and,¹³ biosensor,¹⁴ and antimaterials.¹⁵

Many reports have been devoted to the study of nitrogen bonding in a-CN_x films. In particular, X-ray photoelectron spectroscopy (XPS)^{6,16–26} and vibrational spectroscopy (Raman and FTIR)^{20,21,23,26} measurements have been the most common techniques used to investigate this subject. However, interpretation of these data varies widely in the literature. This is not surprising, since the varieties of different bonding configurations are mostly close in energy to each other. In this respect, one can be faced with interpreting spectra with a multitude of overlapping peaks, which makes deconvolution of curves problematic. C–N_x films deposited by hydrocarbon gas plasma produce polymer-like hydrophobic films rather than crystalline structures and are highly amorphous and inhomogeneous in nature due to the presence of hydrogen in the film surface.²⁷

Major significant obstacles to the synthesis of crystalline β-C₃N₄ are (1) the existence of N–H and C–H_x bonds which are formed in most of the deposition systems and (2) the incorporation of the nitrogen in the carbon layer to reach N/C ≈ 1.33.

In our previous study,²⁸ solid state NMR results do not show a trace of aromatic compound but exhibit the ¹H and ¹³C signals strongly broadened due to homo- and heteronuclear dipolar couplings. It contradicts the results obtained from other published literatures, where it has been mentioned that the films are composed of aromatic compounds such as pyridine, pyridol [2,1,6-de] quinolizine, and so on.^{18,29–31} In the present study, we observed a large shift of the C 1s peak (maximum at N/C = 0.76) toward a higher binding energy state (from 284.94 to 287.4 eV) as the nitrogen concentration is increased in the deposited a-CN_x film. Knowledge of the chemical bonding states of a-CN_x is vital in the development of these applications, since it allows us to design for electronic structure, dielectric properties, and hardness. The structure and chemical bonding states of a-CN_x film are frequently analyzed by X-ray photoelectron spectroscopy (XPS) and FTIR spectroscopy. Many researchers have referred to the chemical bonding states based on the peak deconvolution of the C 1s and N 1s spectra,^{18,32,33,34} However, there have been several differing arguments regarding the deconvolution of these spectra, especially that of N 1s. These disagreements are due to the complexity of the amorphous structure.

In this paper, we present the influence of nitrogen on the chemical bond structure of the a-CN_x film deposited by CH₄/N₂ DBD plasma and also the more precise peak assignments of the a-CN_x film by XPS and FTIR spectra. The quantification of several components obtained by XPS has been compared with the elemental analysis.

* To whom correspondence should be addressed. E-mail: majumdar@physik.uni-greifswald.de. Fax: +493834864701. Phone: +493834864784.

[†] Institute of Physics, Ernst-Moritz-Arndt-University Greifswald.

[‡] Università Magna Græcia di Catanzaro.

[§] Institute for Biochemistry, Ernst-Moritz-Arndt-University Greifswald.

TABLE 1: Samples Number and Dielectric Barrier Discharge Parameters

sample	CH ₄ :N ₂	time (h)	frequency (kHz)
CHN51_24	5:1	24	5.5
CHN31_24	3:1	24	5.5
CHN11_24	1:1	24	5.5
CHN13_24	1:3	24	5.5
CHN15_24	1:5	24	5.5
CHN17_24	1:7	24	5.5
CHN13_07	1:3	7	5.5
CHN13_3.3	1:3	3.3	5.5

II. Experimental Methods

Six films were deposited with varying CH₄:N₂ gas mixture ratios as 5:1, 3:1, 1:1, 1:3, 1:5, and 1:7, respectively (see Table 1). The a-CN_x:H films were deposited on p-type Si(100) substrate which is placed on the ground electrode. The typical time duration of the film deposition is 24 h for all of the deposited CN films. The experimental setup of the dielectric barrier discharge has been explained in detail elsewhere.^{27,28,35} Both of the Ag electrodes are covered by dielectrics: the upper (powered) electrode is covered with aluminum oxide ($\epsilon \sim 10$); the lower (grounded) electrode with a glass plate ($\epsilon \sim 3.8$). Both electrodes were separated by 0.15 cm from each other. A small piece of Si(100) wafer was placed on the glass electrode. The upper electrode is connected to a home-built high voltage power supply, while the lower electrode is grounded. The chamber is pumped by a membrane pump down to about 10 mbar. Pressure inside the plasma chamber was controlled by two gas flow controllers for methane and nitrogen and by an adjustable needle valve between the chamber and the membrane pump. The experiments were performed with the chamber filled at a pressure of 300 mbar and with varying CH₄/N₂ mixture ratios (5:1, 3:1, 1:1, 1:3, 1:5, and 1:7). The amplifier can be operated at up to 500 W. Experiments were performed at 10.5 kV (peak-to-peak) and at 5 kHz. The electrical power under these conditions was 4 W. Table 1 summarizes the deposition conditions.

X-ray photoelectron spectroscopy (XPS) measurements of the a-CN_x:H films were performed on a multitechnique 100 mm hemispherical electron analyzer (CLAM2: VG Microtech), using Mg K α radiation (photon energy 1253.6 eV) as the excitation source and the binding energy (BE) of Au (Au 4f_{7/2}: 84.00 eV) as the reference. The XPS spectra were collected in a constant analyzer energy mode, at a chamber pressure of 10⁻⁸ mbar and pass energy of 23.5 at 0.125 eV/step.

Fourier transform infrared (FTIR) absorption spectra were obtained by means of a FTIR spectrometer (Bruker Vector 22) in transmission mode. The plain sample was placed in a vacuum chamber built inside the spectrometer in order to minimize the IR signal of water vapor, CO₂ content, and noise. The measuring signal passed the optical way with an aperture diameter of 3 mm with a spectral resolution of 4 cm⁻¹. For optimal signal-to-noise ratio, 50 scans were averaged per sample spectrum and apodized by applying the Happ–Genzel apodization function for Fourier transformation. Interferograms were used with a zero-filling factor of 0. The background spectrum was independently measured on a pure silicon substrate.

Elemental analysis was carried out with a CHNS-932 analyzer from LECO using standard conditions.

¹H NMR spectra of CD₃OD soluble film components (roughly 80%) were recorded on a multinuclear FT-NMR spectrometer (Bruker ARX300, 300.1 MHz). The ¹H chemical shifts are in δ values and given in ppm relative to Me₄Si, as internal standards.

Mass spectra (EI, 70 eV) were measured on a single-focusing mass spectrometer (AMD40, Intectra). The film sample obtained with CH₄/N₂ 1:1 was placed in a microcrucible and was heated in a vacuum in the inlet system (push rod) up to 330–350 °C. A substantial total ion current indicating formation of volatile species by thermal decomposition of the film started at ca. 300 °C and became strong at 330 °C. After the measurement at 330 °C, a hard black residue covered the inside surface of the crucible.

III. Results

X-ray Photoelectron Spectroscopy. The best Gaussian distribution function fits to the XPS lines resulted in four different peaks for the C 1s line and three peaks for the N 1s line. In order to minimize interference between the peaks during deconvolution, all spectra have been fitted with equal line widths (full width at half-maximum, fwhm) of the involved individual peaks, thereby reducing the number of free parameters and yielding a more stable result. The investigated C 1s and N 1s spectra display a chemical shift that is caused by an anomalous behavior of the surface charge distribution of the silicon substrate covered by carbon nitride film. Si (2p) with BE = 99.3 eV was taken as a reference.²⁷ We used an a-CN_x film, deposited on a Si substrate, of which a small part of the deposited film had been removed in order to get access to the Si surface. A shift of 4.5 \pm 0.5 eV was noted, which is considered as system calibration. The results presented below have been corrected by subtracting the experimentally observed shift for all of the analysis. The binding energy of C 1s is 284.5 and for N 1s is 398.1 eV, taken as a reference, and with respect to this value, we have calculated the chemical shift of the C 1s and N 1s peaks which have been obtained from experimental results.³⁶

Figure 1 shows the XPS C 1s core-level spectra of a series of a-CN_x films with various methane/nitrogen concentrations. We can observe that the effect of nitrogen incorporation shifted the C 1s peaks toward higher binding energy states (from 284.90 to 286.4 eV) with a maximum shift of 1.88 eV at CH₄/N₂ \sim 1:7. Interestingly, the shifted peaks exhibit an asymmetric broadening toward higher binding energy too. As nitrogen is incorporated, more components are necessary to fit the spectra, indicating that carbon is at least in four different binding states, including one peak for CO bonds. From Figure 1, the carbon peak at the binding energy range 284.00–284.87 eV is identified as originating from adventitious (extrinsic or accidental) carbon and surface carbon that may have lost its nitrogen neighbors due to reaction with O₂ and CO/CO₂ from the air. Similarly, the C 1s peak binding energy range at 287.38–288.92 eV is identified as originating from CO type bonds which are depending on the type of bonding such as ketones/aldehydes (–CO/–CHO), carboxyls (–COOH), and carbonates (–CO₃). The presence of the undesired oxygen in the lower nitrogen content films (at CH₄/N₂ = 5:1 and 3:1) is also effectively responsible for the large binding energy shift. From Figure 1, we can observe that there are two C 1s peaks (second and third) in the ranges 284.94–286.04 eV and 285.93–287.42 eV which are assigned as substitutional sp² N in graphite-like structures (C=N), 3-fold-coordinated N bonded to 4-fold-coordinated sp³ C (C–N) and C \equiv N, respectively.^{18,19,22,25–33}

Figure 2 shows the XPS N 1s core-level spectra of a series of a-CN_x films with various methane/nitrogen concentrations. With increasing N/C ratio, the chemical shift is gradually shifted toward higher binding energy states (from 398.53 to 399.70 eV) with a maximum shift of 1.65 eV at CH₄/N₂ \approx 1:7. The N 1s

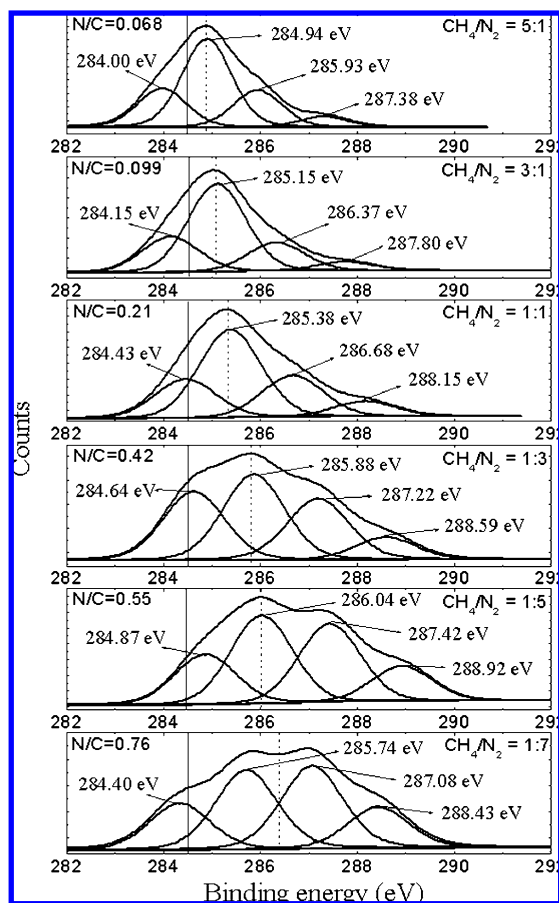


Figure 1. Typical C 1s XPS spectra obtained with Mg K α X-rays at 23.5 eV pass energy at 0.125 eV/step. The data are presented after inelastic background subtraction and using Gaussian fits. The intensity scales for the C spectra are not the same. The straight line denotes the reference binding energy of C 1s at 284.50 eV, and the dotted lines represent the peak position of the deconvoluted area.

peaks are deconvoluted into three components depending on the nitrogen concentration. There are two nitrogen peaks (first and second) in the range 397.88–398.44 eV and from 399.15 to 399.60 eV which are assigned as organic nitriles or isonitriles (R–C \equiv N or R–NC) and methylene imines (R–N=CH–), respectively.^{19,26,30–32} The peak in the range 400.01–400.75 eV is identified as originating from N–O/N–N or nitrosomethane-like (R–N=O) species. At higher binding energy, the corresponding peak can be assigned to NO, as oxygen was detected as a surface contaminant, and may also result from N₂ molecules trapped in the film.^{18,19,22,25–33} From Figure 3, we can observe the non-nitrogenated film (CH₄/Ar = 5:1). The C 1s peak is very sharp (fwhm = 1.5 eV) and is located at 284.67 eV, slightly higher than the value of other pure carbon hydrogen systems. Moreover, at CH₄/N₂ = 5:1 and 3:1, the C 1s peaks are sharper than in other gas mixture ratios. A noticeable change in the sharpness (as well as the binding energy shift) of the C 1s peak is observed while varying the CH₄/N₂ ratio from 1:1 to 1:7. In this paper, we assign the peak at lower binding energy (397.88–398.4 eV) to nitrogen bonded to sp³ carbon and the peak at higher binding energy (399.15–399.60 eV) to nitrogen bonded to sp² carbon following the comparison of the N 1s peak position with reference data from nitrogen containing polymers and organic molecules.^{18,19,22,25–33} However, this contradicts the data obtained from pyromethene which contains N and C atoms but no sp³ carbon.^{25,26} Nevertheless, Souto et al.³² recently compared the valence and core level electronic structures of

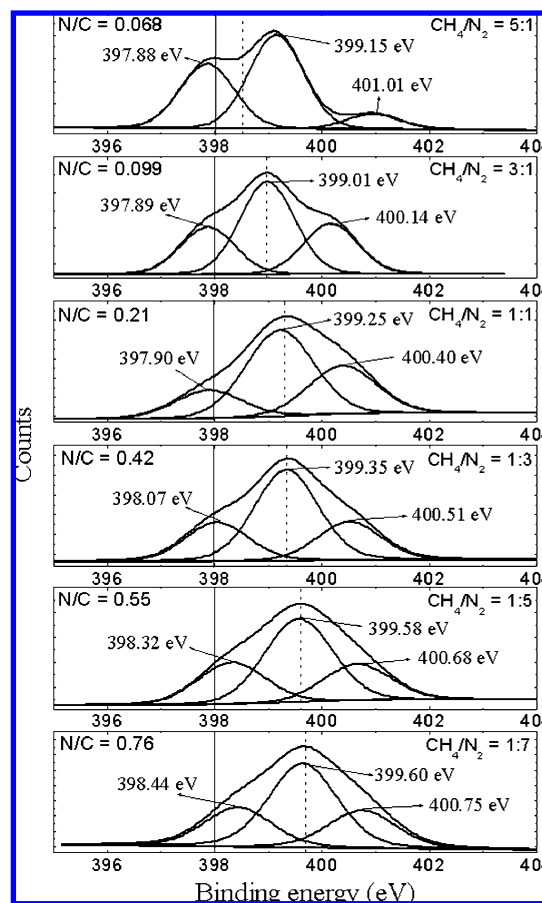


Figure 2. Typical N 1s XPS spectra obtained with Mg K α X-rays at 23.5 eV pass energy at 0.125 eV/step. The data are presented after inelastic background subtraction and using Gaussian fits. The intensity scales for the N spectra are not the same. The straight line denotes the reference binding energy of N 1s at 398.01 eV, and the dotted line presents the peak position of the deconvoluted area.

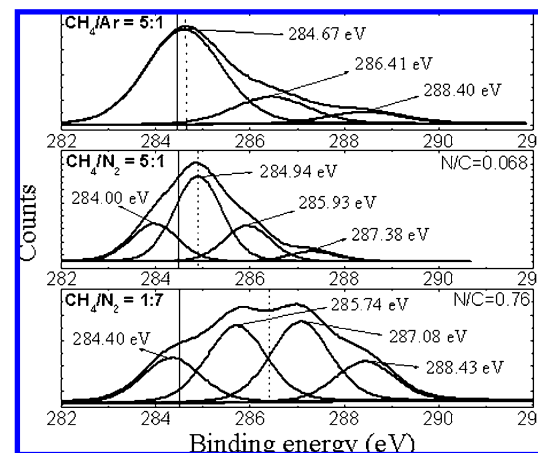


Figure 3. Comparative study between non-nitrogenated (CH₄/Ar = 5:1) and nitrogenated (CH₄/N₂) films with respect to the C 1s peak shifting toward higher binding energy region. The film deposited by CH₄/Ar composition proposed \approx 0.15 eV shift in C 1s peak, as it is 0.94 and 2.90 eV in the case of CH₄/N₂ = 5:1 and 1:7, respectively. The intensity scales are not the same for all C 1s spectra. The straight line denotes the reference C 1s binding energy at 284.50 eV, and the dotted lines represent the peak position of the deconvoluted area.

sputtered a-CN_x films with a theoretically calculated density of states and core level binding energies of molecules containing sp²/sp³ CN bonds. The combined analysis of core level and valence band spectra leads to the conclusion that the peak at

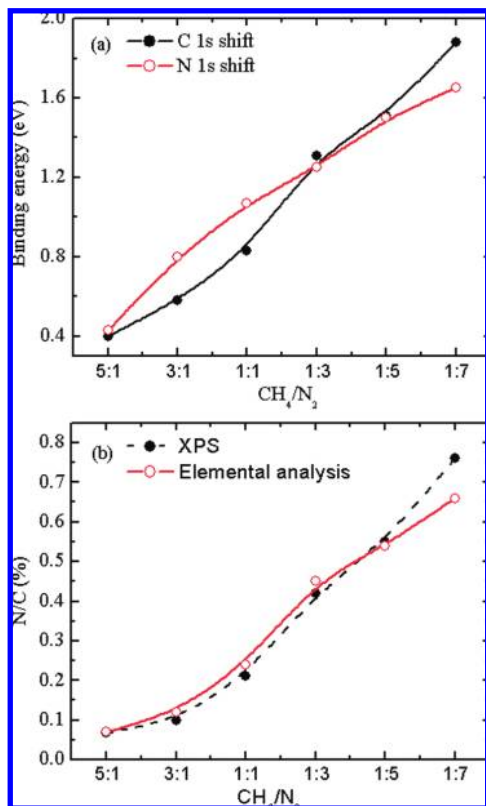


Figure 4. (a) Shift in binding energy of C 1s and N 1s with respect to CH₄/N₂ gas composition of a-CN_x films and (b) comparative study of N/C obtained from XPS and elemental analysis as a function of CH₄/N₂ gas ratio.

TABLE 2: Chemical Shift of the Corresponding Deposited Films with Different CH₄/N₂ Compositions and N/C Ratios

sample	CH ₄ :N ₂	N/C (XPS)	N/C (elemental)	C 1s peak shift (eV)	N 1s peak shift (eV)
CHN51_24	5:1	0.068	0.07	0.40	0.43
CHN31_24	3:1	0.099	0.12	0.58	0.80
CHN11_24	1:1	0.21	0.24	0.83	1.07
CHN13_24	1:3	0.42	0.45	1.31	1.25
CHN15_24	1:5	0.65	0.54	1.51	1.50
CHN17_24	1:7	0.76	0.66	1.88	1.65
CHN13_07	1:3	0.30	0.32	1.28	1.18
CHN13_3.3	1:3	0.22	0.20	1.27	1.19

lower energy is related to N atoms in configurations with isolated lone pairs (including 3-fold-coordinated N atoms bonded to sp³ carbon), while the peak at higher binding energy corresponds to substitution of N in graphite-like configurations, where the lone pairs are involved in stronger π -bonds (this includes N atoms bonded to sp² C).

In the assumed β -C₃N₄ structure, the carbon atoms are in tetrahedral sites and the nitrogen atoms are in a 3-fold position. The tetrahedral allotrope of carbon has about the same binding energy as other pure carbon forms and hydrogenated carbons.^{37,38} Figure 4a plotted as taking data from Table 2 shows the dependence of the C 1s binding energy on the nitrogen content can be considered as a result of the chemical shifts on charge transfer.⁹ Furthermore, from Figure 4b, the N/C ratio obtained from XPS and elemental analysis are significantly supported by each other except for a small deviation of ± 0.22 eV. The gradual increase of asymmetry of the C 1s line is consistent with the broadening of the C 1s line. It is understood from XPS results that the environment of carbon is becoming more

heterogeneous with the increase of nitrogen concentration in the films, mainly due to the formation of CN bonds.

In particular cases, the presence of a first and second order amine/ amide group strongly determines the polarity of the deposited a-CN_x films as well as the binding energy shift. The incorporation of nitrogen in the a-C:H_x matrix induces a charge transfer from the less electronegative C (2.5)²⁰ atoms to the more electronegative N (3.04) atoms. This decrease in the electron density on the C atoms results in a shift of all C core levels toward higher binding energies, as more homopolar C–C bonds are replaced by heteropolar C–N bonds. From Figures 1, 2, and 3, it is confirmed that the presence of hydrogen introduces a component in a position of intermediate peaks that are usually well resolved for non-hydrogenated CN films. The assignment of those peaks is controversial, mainly because CN polymers and organic molecules are used as reference materials, which are poor conductors and no reliable binding energies have been assigned. In some cases, it is difficult to distinguish between different carbon configurations referring to sp² or sp³ CN bonds¹⁸ and in fact there is no evidence for a significant difference in the C 1s positions between graphite and diamond. Thus, it is more likely that the different binding energies correspond to a difference in the number of nitrogen neighbors.¹⁹

FT-IR Absorption Spectroscopy. FTIR absorption spectra were carried out in the range 4000–1000 cm⁻¹ for all of the a-CN_x samples, deposited by the DBD technique. Figure 5 shows the FTIR spectra for the a-CN_x samples by varying the nitrogen. The samples are categorized in three groups: (a) by varying the N₂ gas pressure and keeping methane gas pressure and deposition time constant, (b) by altering the methane gas pressure and keeping the N₂ gas pressure and deposition time constant, and (c) by changing the film deposition time only.

Various absorption bands are observed in the ranges 3750–2650, 2295–2080, 1835–1495, and 1480–1365 cm⁻¹, associated with the combination of O–H, N–H, and C–H_x stretching,^{23,27,28} C≡N stretching, C=N stretching, and C–H_x bending vibration, respectively. The C=N band at 1655 cm⁻¹ might be superimposed by the C=O stretching band of amide (CONH) which absorbs in the same range and would fit with the CO bands detected by UPX analysis. NH of associated amide will in turn be superimposed by OH/NH bands. Figure 5a shows that, as the nitrogen pressure increases, there is an increase in C≡N bond formation (consequently, an increase in nitrile/isonitrile band intensity) and, simultaneously, a decrease in C–H_x band intensity. Thus, it seems that, when a more electronegative element (e.g., nitrogen) interacts with the methane, it leads to the formation of nitrile/isonitrile groups at the expense of C–H_x groups. This is clearly observed in the inset of Figure 5a. A strange finding results in the extreme case when the CH₄:N₂ ratio was 1:7. In this case (CN17_24), the intensity of the nitrile/isonitrile absorption is almost equal to that of CHN11_24. It seems that, when saturation of C≡N group formation is reached, the deposited material starts to decompose. The reason behind this hypothesis is that, with the decrease of the C≡N bands, there is an increase of the C=N band centered at about 1655 cm⁻¹.

In the case of sample deposition by varying the methane/N₂ gas composition, it is found that just after increasing the methane gas pressure the C–H_x band intensity reaches saturation. FTIR absorption spectra are illustrated in Figure 5b. It is clearly observed that the C–H_x bands are intense while the C≡N group vibrational bands are weak. The nitrile/isonitrile band region is shown in the inset of Figure 5b. However, when there is a ratio of 1:1 for CH₄:N₂, the C≡N group absorption becomes stronger

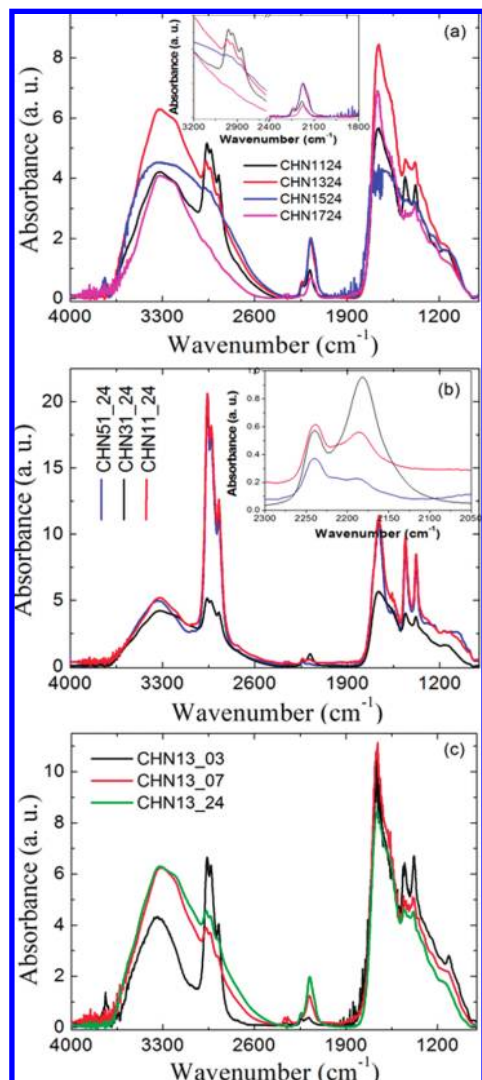


Figure 5. FTIR spectra in the range 4000–900 cm^{-1} by (a) varying the nitrogen pressure and keeping the other deposition parameters constant, (b) changing the methane gas pressure and keeping other parameters invariable, and (c) varying only the time of deposition.

as it is reduced with the increase of the methane content and is found a minimum in the case of the CHN51_24 sample. There are various bands related to $\text{C}\equiv\text{N}$ groups, 2177–2185, 2214, and 2240 cm^{-1} , which might be attributed to the nitrile ($-\text{C}\equiv\text{N}$) group attached to a $\text{C}=\text{O}$ group, $-\text{C}\equiv\text{N}$ conjugated to a $\text{C}=\text{C}$ group, and $-\text{C}\equiv\text{N}$ linked with an alkyl group, respectively.²⁴ Alternatively, the band at 2177–2185 cm^{-1} , in the CHN11_24 film ($\text{CH}_4/\text{N}_2 = 1:1$) in KBr observed at 2174 cm^{-1} , might be attributed to isonitrile groups. Isonitriles absorb bathochromically shifted vs nitriles due to the slightly lower bond order, in the VB model expressed by a neutral carbene resonance structure with $\text{C}=\text{N}$ bond ($\text{R}-\text{N}=\text{C} \leftrightarrow$). Isonitriles are less stable than nitriles and can rearrange to the latter but are formed primarily in reactions of cationic alkyl species with cyanide anions^{39,40} and may thus be formed under plasma conditions. The broad-band with peaks centered at about 3325 cm^{-1} and about 3200 cm^{-1} is related to the $\text{N}-\text{H}$ vibrational bands in different configurations.^{27,28}

An interesting behavior is observed by changing the deposition time of the a-CN_x samples by keeping the CH_4/N_2 flux ratio 1:3, shown in Figure 5c. It is observed that an increase in deposition time causes a decrease of the intensity of the $\text{C}-\text{H}_x$ bands and simultaneously enhances the $\text{C}\equiv\text{N}$ bond formation.

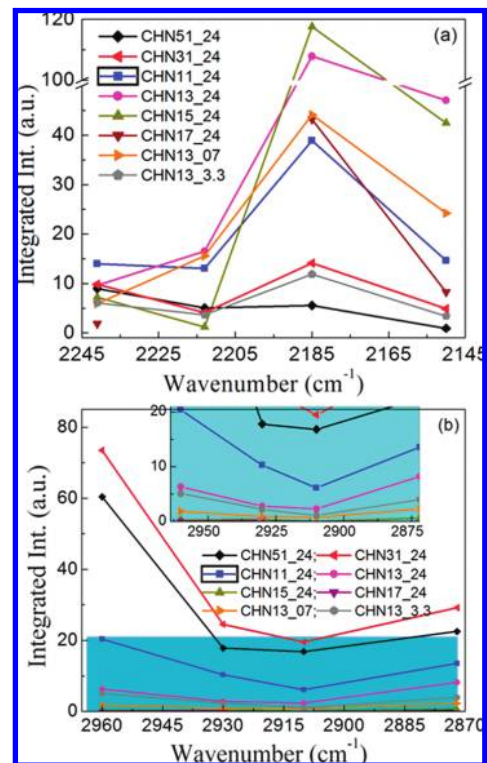


Figure 6. Integrated intensity plot for all of the major peaks: (a) in the range 2245–2145 cm^{-1} ; (b) in the range 2965–2870 cm^{-1} . In the inset of part b, the zoomed area of lower integrated intensity is illustrated.

A sharp decrease in $\text{C}-\text{H}_x$ band intensity is observed for 7 h deposition time; then, it remains almost the same. However, further increase in deposition time up to 24 h leads to an increase of $\text{C}\equiv\text{N}$ group formation.

The detailed analysis is performed by carrying out curve fitting using a mixed distribution function ($M \cdot G + (1 - M) \cdot L$); M is the weight function, G is the Gaussian distribution function, and L is the Lorentzian distribution function. The integrated intensities of various bands, $\text{C}\equiv\text{N}$ and $\text{C}-\text{H}_x$, are shown in Figure 6. In general, it is found that the intensity of the $\text{C}\equiv\text{N}$ group at 2185 cm^{-1} is higher with respect to the alkylnitrile absorption. The alkylnitrile band centered at around 2240 cm^{-1} is higher only for the CHN51_24 sample. For all of the samples, various stretching vibrational bands of $\text{C}-\text{H}_x$ are observed centered at 2960, 2930, 2910, and 2872 cm^{-1} which are attributed to the $\text{sp}^3\text{-}\nu\text{CH}_3$, $\text{sp}^3\text{-}\nu\text{CH}_2$, $\text{sp}^3\text{-}\nu\text{CH}$, and $\text{sp}^3\text{-}\nu\text{CH}_3$, respectively.^{41,42} The integrated intensity for the $\text{C}-\text{H}_x$ stretching vibrational bands in various configurations is plotted in Figure 6b. A zoomed area is shown in the inset of Figure 6b for better illustration of the low integrated intensity region. It is observed that the integrated intensity of the $\text{C}-\text{H}_3$ vibrational band is always higher than other $\text{C}-\text{H}_x$ ($x = 1-2$) bands, which suggests major contributions of CH_3 species within the $\text{a-CN}_x\text{:H}$ sample.

Elemental Analysis, NMR, and Thermolysis Mass Spectrometry. From Figure 4, it is seen that the N/C ratio obtained from the elemental analysis is fitting well with the XPS analysis. The elemental analysis of the CHN11_24 film ($\text{CH}_4/\text{N}_2 = 1:1$) removed from the glass electrode is (in wt %) C 67.68, H 9.88, N 16.53. After summing up these values (94.09%), it is clear that there is something more in the film, other than C, H, or N. The remaining 5.91 wt % of the sample probably belongs to oxygen. The IR vibrations in the higher frequency region at

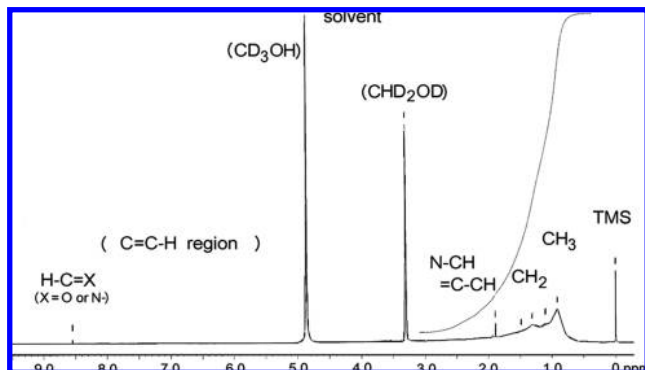


Figure 7. ¹H NMR spectrum of the CD₃OD extract of CHN11_24 film (CH₄/N₂ = 1:1) recorded at 300.1 MHz (TMS as internal standard) showing broad proton signals for CH₃, –CH₂, X=C–CH₂, and N–CH_x at δ 0.6–2.4 but no alkenyl or aryl C=C–H proton signals.

around 3330 cm⁻¹, assigned partly to ν_{O–H}, and the XPS bands assigned to C=O species as discussed above, are supporting the existence of oxygen in the film, possibly due to absorption of moisture from air by reactive sites of the film. Thus, the final film is made up of the elements C, H, N, and O. The fractional empirical formula directly from elemental analysis and calculated by the elemental weight of carbon, hydrogen, and nitrogen is C_{5.6}H_{9.8}N_{1.2}O_{0.4}.

To get further information on the structural units included in the film material, the solubility in various NMR solvents was tested (insoluble in most solvents, sparingly soluble in methanol), and a CD₃OD extract, prepared by irradiating with ultrasound, was measured by ¹H and ¹³C NMR with an internal standard of tetraethyl silane (TMS). The ¹H NMR spectrum shows superimposed broad peaks in the range δ 0.55–2.25 ppm with maxima at 0.90, 1.10, and 1.30 ppm, assigned to –CH₃ and –CH₂ groups, respectively (Figure 7). Assuming roughly equal overlap of CH₃ and CH₂ signals, the integration hints to a proton ratio of about 1:2, i.e., on average, three CH₂/CH₃ groups. The broad low intensity absorption from δ 1.5–2.2 ppm may be attributed to superimposed sp³-CH–C=C, sp³-CH_x–C=N sp³-CH_x–C≡N (x = 1 or 2), or sp³-CH_x–N(sp^{1–3}) structural units. The lack of fine splitting does not allow conclusions on the connectivity of these structural units. The absence of peaks in the region from δ 2.5 to 8.0 ppm except solvent signals and a tiny singlet at δ 8.55 ppm, probably a formyl group (H–C=O), indicates that the soluble part of the film has no aromatic and vinyl =CH groups. This fact is also evident from the IR spectra by the absence of the indicative =CH out-of-plane deformation bands in the region 665–995 cm⁻¹. Attempts to get information on quaternary sp³-C, sp²-C, and sp-C atoms without protons or closer details on the microstructure of the alkyl groups by ¹³C NMR failed, even after collecting 56 320 scans. Only a raised wavy basis line within the upper noise level hints to very broad and flat bands in the alkyl range. Possibly radical centers are present which prevent sharp signals. The occurrence of linear and weakly methyl branched alkyl groups with (iso)nitrile end groups can however be derived from the thermolysis mass spectrum. Heating the CHN11_24 film material (from CH₄/N₂ = 1:1) in an aluminum crucible, placed in the push rod of the mass spectrometer, showed a substantial total ionic current when reaching around 300 °C and a strong current at 330 °C. This indicates thermal decomposition of the film and cleavage of groups which are less firmly bound at the film polymer and give rise to molecular and fragment cations (EI 70 eV). The residue left after heating formed a black hard layer on the inner

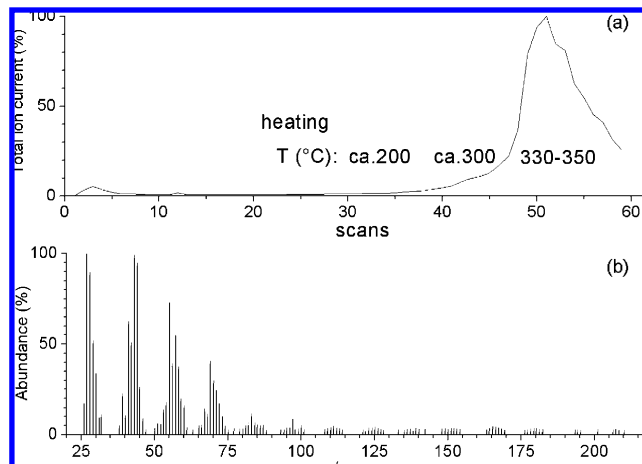


Figure 8. Thermolysis mass spectrum of the CHN11_24 film (CH₄/N₂ = 1:1): (a) temperature dependence of the total ionic current; (b) mass spectrum of the volatiles cleaved at 330 °C from the film material. The base peak *m/e* 27 (CNH⁺) and repeated fragment distances Δ*m/e* 14 (CH₂) hint at –(CH₂)_n–CNH⁺ ions, i.e., cleavage of less firmly (single) bound alkyl(iso)nitrile groups from the film as a major process in the thermal decomposition.

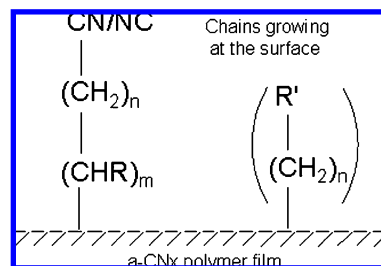


Figure 9. Alkyl(iso)nitrile structural units detected in the CHN11_24 film (CH₄/N₂ = 1:1) by ¹H NMR of CD₃OD soluble parts and thermal cleavage of less firmly (single) bound groups (*n* = 0–3 in abundant peaks, *n* = 4–8, and R = H, Me, *m* = 0–2 in weak peaks). R' is uncertain and might be H, C(O)NH₂, or NCHO (e.g., from addition of H₂O at reactive isonitrile groups). It is suggested that these groups grow at the surface and are gradually converted to polymer during DBD plasma exposure.

surface of the crucible. The mass spectrum of the cleaved volatiles displayed *m/e* 27 (HCN⁺) as the base peak, followed by strong peaks at *m/e* 41, 55, and 69 and weak peaks at *m/e* 83, 97, 111, 125, and 139 (Δ*m/e* = 14, CH₂), each forming the maximum of wave-shaped peak clusters (Figure 8). The distance to the maxima of the next small peak groups is 13 and then 15, attributable to sp³-CH of branching sites (by lack of hints at =CH in ¹H NMR) and CH₃, respectively. These findings represent a series –(CH₂)_n–CN/NC+H⁺ with strong peaks for *n* = 0–3 and weak peaks for *n* = 4–8 as well as few additional CHMe units in place of CH₂. These observations suggest that the film is made up of a nonvolatile polymeric a-CN_x:H basis material containing aliphatic substituents with (iso)nitrile end groups. At least a part of these groups has CHMe units at the end opposite the (iso)nitrile group (Figure 9). More or less long fragments of these groups may be cleaved off during thermolysis to give the observed peak pattern. The other strong peaks at *m/e* 43, 44, and 57 may be due to propyl, propane, and butyl cations and/or to amide (–(CH₂)_n–CONH₍₂₎⁺; *n* = 0,1), imine or formyl species (–(CH₂)_n–CH₂=XH⁺; X = NH, O, *n* = 1,2), or CO₂⁺ (for *m/e* 44). Thus, additional short amido-, imino-, or carboxy-alkyl end groups at the polymer bulk are also possible. Species with a relatively high ratio of substituents per polymer form probably the CD₃OD soluble part observable in ¹H NMR.

IV. Discussion

As found typically for a-CN_x films in the literature,^{6,9,18,19,22,25–33} the C 1s spectrum exhibits four peaks which are located at (1) around 284.5 eV for sp² C in graphite-like structures (C=C), (2) around 285.55 eV for substitutional sp² N in graphite-like structures (C=N), (3) around 286.5 eV for 3-fold-coordinated N bonded to 4-fold-coordinated sp³ C (C–N) and C≡N, and (4) around 288–290 eV for C–O bonds. Similarly, the N 1s spectrum exhibits three peaks which are located at (1) 398.2–398.6 eV, (2) 399–399.8 eV, and (3) 400–402.5 eV and have been assigned to C–N/C≡N, C=N, and N=O or N=N, respectively.^{6,9,18,19,22,25–33} There is a significant difference between most organic and inorganic compounds regarding chemical shift in photoelectron spectroscopic measurement. In a very simple model, it is assumed that the electrons are completely transferred from the element with lower to that with higher electronegativity.^{9,20} This is an oversimplification, since when the difference in electronegativity is small the bond has an appreciable covalent character. A simple refinement of the model is to assume that the bond is entirely ionic if the difference in electronegativity is larger than 0.5 and entirely covalent if the difference is smaller than 0.5 (in which case only one-half of the charge in the ionic model is transferred). For a-CN_x films, the difference in electronegativity is approximately 0.54 (Pauling scale) (3.04 (N) – 2.5 (C) ≈ 0.54). In the above model, the film is slightly inclined toward polar bonds (–C⁺≡N[–]). With respect to N–H bonds, the electronegativity difference is 0.84 (Pauling scale; 3.04 (N) – 2.2 (H) ≈ 0.84), which indicates the more ionic, strongly polar properties (H⁺–N[–]). The total polarity (percent ionic character) strongly depends on the N/C ratio.

Hydrogen atoms cleaved from methane or alkyl groups of the film may attack and break or change the C≡N bond and form C–H and N–H bonds. This behavior is strongly undesirable from the viewpoint of obtaining crystalline β-C₃N₄. In the ideal network structure of CN_x, nitrogen would always be fully coordinated by three carbon atoms. In this case, no chemical conversions with changes in concentration can be expected. The perfect carbon nitride, β-C₃N₄ or α-C₃N₄, has been considered as an extremely stable material, which hardly reacts with any gas or other chemical at room temperature. Unstable carbon nitride films, however, react with hydrogen under plasma conditions, and then C≡N or C=N bonds break and are converted to C–H and N–H bonds.⁴¹ They also contain a high concentration of dangling bonds, which cause the deviations in interatomic spacing^{1–5} of more than 5%, and noticeable variation in bond angle. However, FTIR spectroscopy showed the presence of hydrogen in the a-CN_x:H network in the form of N–H bonds (in addition to the formation of C=N bonds) with increasing N incorporation. These results are interpreted in terms of an atomic structure consisting of a carbon backbone surrounded by a nitrogen and H layer.^{43,44} The formation of polarizable C=N bonds increases the negative charge at the N atoms and induces the formation of an asymmetric shoulder toward lower binding energies. In the case of paracyanogen (C=N)_n, the carbon atom can add two hydrogen atoms (per unit) to become stabilized. In turn, C–H and N–H bonds formed in advance can return C≡N and/or C=N bonds. Therefore, hydrogen-defected carbon nitride films can provide dangling sites to capture water molecules physically or chemically. Figure 9 shows the proposed molecular structure of the deposited polymer film of CHN11_24 film (CH₄/N₂ = 1:1), which has been established from the combination of XPS and elemental analysis, FTIR, NMR, and thermolysis mass spectrometry. It

can be expected that the other deposited films contain similar linear groups at the CN_x polymer, possibly with changed ratio of CN containing and nitrogen free alkyl groups and varying chain lengths depending on the wt % of C, N, and H. More intense methyl signals may mean a relatively higher content of (CH₂)_n–R' with *n* = 1 and R' = H (Figure 9). Finally, because chemical polymerization of isonitriles to insoluble, nonmelting polymers is known,^{45,46} the detection of volatile alkyl(iso)nitrile moieties cleaved from the polymer puts the question, if the nonvolatile a-CN_x:H basis material may result from primary formed alkylisonitriles by polymerization in the DBD plasma. To answer this question would be a challenging task for further investigations on the mechanism of a-CN_x:H deposition in DBD plasma.

V. Conclusions

In conclusion, we propose that the hydrogenated carbon nitride (a-CN_x:H) film deposited by CH₄/N₂ DBD plasma is composed of polymeric a-CN_x, which is substituted by linear alkyl(iso)nitrile, short alkyl, and some other groups. Complementary elemental analyses satisfactorily support the results obtained from XPS with respect to elemental composition and N/C ratio. FTIR spectra suggest that the majority of the incorporated nitrogen atoms belong to C=N, possibly also some primary amide (CONH₂, same band range), N–H, C≡N (nitrile/isonitrile), and C–N bonds. CH₂/CH₃ bands in IR in combination with thermolysis mass spectrometry of the film and ¹H NMR signals for aliphatic residues in the soluble parts hint at saturated alkyl chains with nitrile and isonitrile end groups as part of the film material. These moieties may represent intermediate growing species which convert to the polymeric material during exposure to DBD plasma.

Acknowledgment. Part of this work was supported by the Federal Ministry of Education and Research (BMBF) through Verbundprojekt “Campus PlasmaMed”, by the Deutsche Forschungsgemeinschaft (DFG) through Sonderforschungsbereich SFB/TR24 “Fundamentals of Complex Plasmas”, and by The International Max-Planck Research School (IMPRS) “Bounded Plasmas”. Thanks to Mr. Sadhan Das, IUC-DAEF, Indore, India, for several discussions and M. Steinich (Greifswald) for measuring NMR and mass spectra.

Note Added after ASAP Publication. This paper was published ASAP on November 6, 2009. In the Results section, a reference to Figure 4a was changed to Figure 5a. The updated paper was reposted on November 11, 2009.

References and Notes

- (1) Cohen, M. L. *Phys. Rev. B* **1985**, *32*, 7988.
- (2) Liu, A. Y.; Cohen, M. L. *Science* **1989**, *245*, 841.
- (3) Teter, D. M.; Hemley, R. J. *Science* **1996**, *271*, 53.
- (4) Niu, C.; Yuan, L. Z.; Lieber, C. M. *Science* **1993**, *261*, 334.
- (5) Sjöström, H.; Stafström, S.; Boman, M.; Sundgren, J. E. *Phys. Rev. Lett.* **1995**, *75*, 1336.
- (6) Hellgren, N.; Johansson, M. P.; Broitman, E.; Hultman, L.; Sundgren, J. E. *Phys. Rev. B* **1999**, *59*, 5162.
- (7) Li, D.; Chung, Y. W.; Wong, M. S.; Sproul, W. D. *J. Appl. Phys.* **1993**, *74*, 219.
- (8) Yao, H.; Ching, W. Y. *Phys. Rev. B* **1994**, *50*, 11231.
- (9) Mansour, A.; Ugolini, D. *Phys. Rev. B* **1993**, *47*, 10201.
- (10) Robertson, *Thin Solid Films* **2001**, *383*, 81.
- (11) Zambov, L. M.; Popov, C.; Abedinov, N.; Plass, M. F.; Kulisch, W.; Gotszalk, T. *Adv. Mater.* **2000**, *12*, 656.
- (12) Wang, J.; Miller, D. R.; Gillan, G. *Chem. Commun.* **2002**, *19*, 2258.
- (13) Plass, M. F.; Popov, C.; Ivanov, B.; Mandl, S.; Jelinek, M.; Zambov, L. M. *Appl. Phys. A* **2001**, *72*, 21.
- (14) Lee, S. P. *Sensors* **2008**, *8*, 1508–1518.

- (15) Majumdar, A.; Schröder, K.; Hippler, R. *J. Appl. Phys.* **2008**, *104*, 074702.
- (16) Gammon, W. J.; Kraft, O.; Reilly, A. C.; Holloway, B. C. *Carbon* **2003**, *41*, 1917.
- (17) Holloway, B. C.; Kraft, O.; Shuh, D. K.; Nix, W. D.; Kelly, M.; Pianetta, P.; Hagstrom, S. *J. Vac. Sci. Technol., A* **2000**, *18*, 2964.
- (18) Marton, D.; Boyd, K. J.; Al-Bayati, A. H.; Todorov, S. S.; Rabalais, J. W. *Phys. Rev. Lett.* **1994**, *73*, 118.
- (19) Ronning, C.; Feldermann, H.; Merk, R.; Hofsass, H.; Reinke, P.; Thiele, J. U. *Phys. Rev. B* **1998**, *58*, 2207.
- (20) Kaufman, J. H.; Metin, S.; Saperstein, D. D. *Phys. Rev. B* **1989**, *39*, 13053.
- (21) Chowdhury, A.; Cameron, D. C.; Hashmi, M. S. J. *Thin Solid Films* **1998**, *332*, 62.
- (22) Kusano, Y.; Christou, C.; Barber, Z. H.; Evetts, J. E.; Hutchings, I. M. *Thin Solid Films* **1999**, *355*, 117.
- (23) Mariotto, G.; Das, G.; Quaranta, A.; Mea, D. G.; Corni, F.; Tonini, R. *J. Appl. Phys.* **2005**, *97*, 113502.
- (24) Lin-Vien, D.; Colthup, N. B.; Fateley, W. C.; Grasselli, J. G. *The Hand book of Infrared and Raman Characteristic Frequencies of Organic Molecules*. Academic Press: New York, 1991.
- (25) Zheng, W. T.; Yu, W. X.; Li, H. B.; Wang, Y. M.; Cao, P. J.; Jin, Z. S.; Broitman, E.; Sundgren, J. E. *Diamond Relat. Mater.* **2000**, *9*, 1790.
- (26) Rodil, S. E.; Ferrari, A. C.; Robertson, J.; Milne, W. I. *J. Appl. Phys.* **2001**, *89*, 5425.
- (27) Majumdar, A.; Schäfer, J.; Mishra, P.; Ghose, D.; Meichsner, J.; Hippler, R. *Surf. Coat. Technol.* **2007**, *201*, 6437.
- (28) Majumdar, A.; Scholz, G.; Hippler, R. *Surf. Coat. Technol.* **2009**, *203*, 2013.
- (29) Ripalda, J. M.; Roman, E.; Diaz, N.; Galan, L.; Montero, I.; Comelli, G.; Baraldi, A.; Lizzit, S.; Goldoni, A.; Paolucci, G. *Phys. Rev. B* **1999**, *60*, R3705.
- (30) Bhattacharyya, S.; Cardinaud, C.; Turban, G. *J. Appl. Phys.* **1998**, *83*, 4491.
- (31) Ohta, R.; Lee, K. H.; Saito, N.; Inoue, Y.; Sugimura, H.; Takai, O. *Thin Solid Films* **2003**, *434*, 296–302.
- (32) Souto, S.; Pickholz, M.; dos Santos, M. C.; Alvarez, F. *Phys. Rev. B* **1998**, *57*, 2536.
- (33) Bhattacharyya, S.; Hong, J.; Turban, G. *J. Appl. Phys.* **1998**, *83*, 3917.
- (34) Tabbal, M.; Merel, P.; Moisa, S.; Chaker, M.; Ricard, A.; Moisan, M. *Appl. Phys. Lett.* **1996**, *69*, 1698.
- (35) Majumdar, A.; Hippler, R. *Rev. Sci. Instrum.* **2007**, *78*, 075103–075108.
- (36) Moulder, J. F.; et al. *Handbook of X-ray Photoelectron Spectroscopy*; Perkin-Elmer Corporation: Eden Prairie, Minnesota, 1992.
- (37) Mcfeele, F. R.; Kovwalczyk, S. P.; Ley, L.; Cavell, R. G.; Pollak, R. A.; Shirley, D. A. *Phys. Rev. B* **1974**, *9*, 5268.
- (38) Kasi, S. R.; Kang, H.; Rabalais, J. W. *J. Chem. Phys.* **1988**, *88*, 5914.
- (39) Becker, H. G. O.; Berger, W.; Domschke, G. *Organikum*, 22nd ed.; Wiley-VCH: Weinheim, Germany, 2004; pp 222–256.
- (40) Grundmann, C. In *Methoden der organischen Chemie (Houben-Weyl)*, 4th ed.; Falbe, J., Ed.; Thieme: Stuttgart, Germany, 1985; Vol. VIII, E5, pp 1611–1641.
- (41) Das, G.; Bettotti, P.; Ferraioli, L.; Raj, R.; Mariotto, G.; Pavesi, L.; Soraru, G. D. *Vib. Spectrosc.* **2007**, *45*, 61.
- (42) Mutsukura, N.; Inouse, S.-I.; Machi, Y. *J. Appl. Phys.* **1992**, *72*, 43.
- (43) Han, H.-X.; Feldman, B. J. *Solid State Commun.* **1998**, *65*, 921.
- (44) Crunteanu, A.; Charbonnier, M.; Romand, M.; Vasiliu, F.; Pantelica, D.; Negoita, F.; Alexandrescu, R. *Surf. Coat. Technol.* **2000**, *125*, 301.
- (45) Grundmann, C. In *Methoden der organischen Chemie (Houben-Weyl)*, 4th ed.; Falbe, J., Ed.; Thieme: Stuttgart, Germany, 1985; Vol. VIII, E5, p 1647.
- (46) Arshady, R.; Zecca, M.; Corain, B. *React. Polym.* **1993**, *20*, 147–73.

JP906654M